JACS
JOURNAL OF THE AMERICAN CHEMICAL SOCIETY

COMMUNICATION

pubs.acs.org/JACS

Substituent Effects on Cobalt Diglyoxime Catalysts for Hydrogen Evolution

Brian H. Solis and Sharon Hammes-Schiffer*

Department of Chemistry, 104 Chemistry Building, Pennsylvania State University, University Park, Pennsylvania 16802, United States

Supporting Information

ABSTRACT: The design of efficient, robust, and inexpensive hydrogen evolution catalysts is important for the development of renewable energy sources such as solar cells. Cobalt diglyoxime complexes, $Co(dRgBF_2)_2$ with substituents R, are promising candidates for such electrocatalysts. The mechanism for hydrogen production requires a series of reduction and protonation steps for various monometallic and bimetallic pathways. In this work, the reduction potentials and pK_a values associated with the individual steps were calculated for a series of substituents. The calculations revealed a linear relation between the reduction potentials and pK_a values with respect to the Hammett constants, which quantify the electron donating or withdrawing character of the substituents. Additionally, the reduction potentials and pK_a values are linearly correlated with each other. These linear correlations enable the prediction of reduction potentials and pK_a values, and thus the free energy changes along the reaction pathways, to assist in the design of more effective cobaloxime catalysts.

The design of hydrogen evolution catalysts from earth-abundant materials is important for the development of renewable energy sources such as solar cells. Substantial efforts are currently being directed toward the design of efficient and environmentally benign electrocatalysts that operate at low overpotentials. Cobalt diglyoxime complexes have been shown to produce molecular hydrogen from protic solutions at relatively modest overpotentials.[1−4] Mechanistic studies indicate several possible monometallic and bimetallic pathways, as depicted in Scheme 1.[1−9] The relative probabilities of these pathways depend on the strength and concentration of the acid, as well as the redox properties of the cobaloxime catalyst. In all of these pathways, hydrogen evolution proceeds after an initial reduction of Co^{II} to Co^{I}. The reaction continues through a series of protonation and reduction steps to generate a cobalt hydride that produces molecular hydrogen through a monometallic or bimetallic mechanism. The free energy changes along the reaction pathways depend on the reduction potentials and pK_a values associated with these steps. Because hydrogen evolution typically occurs at an overpotential near the $Co^{II/I}$ reduction potential in electrochemical experiments,[2,4,5,7] the ability to tune the $Co^{II/I}$ reduction potential by altering the substituents on the diglyoxime ligands is important for the design of more efficient catalysts.[2] Tuning the reduction potentials and pK_a values of the cobalt hydride intermediates provides additional flexibility for catalyst design.

Scheme 1. Three Monometallic (A) and Three Bimetallic (B) Pathways for Cobaloxime Catalysts

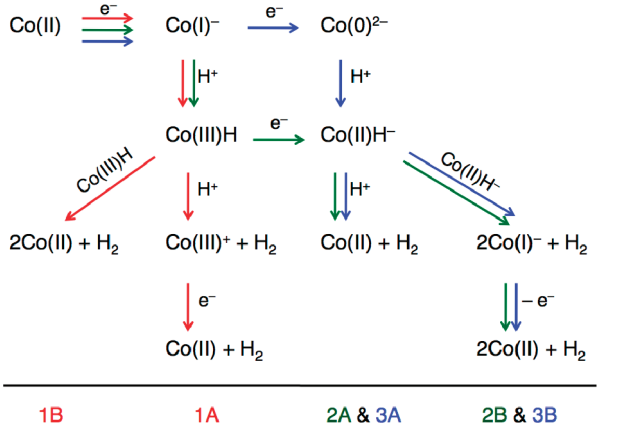

In this work, we calculated the $Co^{III/II}$, $Co^{II/I}$, $Co^{III/II}H$, and $Co^{I/0}$ reduction potentials and the $Co^{II}H$ and $Co^{III}H$ pK_a's for nine different diglyoxime substituents R on the cobaloxime catalyst $Co(dRgBF_2)_2$, which is depicted in Figure 1. We focused on BF_2-bridged complexes because they have been shown experimentally to be more resistant to degradation in acidic solutions than are H-bridged cobaloximes.[1,2] We related the reduction potentials and pK_a's of these complexes to the electron donating or withdrawing character of their substitutents. The electron donating or withdrawing character is quantified in terms of the Hammett constant σ_p, where more negative (positive) values of σ_p are associated with the more electron donating (withdrawing) substituents.[10] The substituents and their associated Hammett constants are given in Table 1. We observed a linear dependence of the reduction potentials and pK_a's with respect to the Hammett constants as well as linear correlations among these properties. These linear correlations enable the prediction of reduction potentials and pK_a's for cobaloximes that have not been studied experimentally and elucidate trends that can assist in the design of more effective hydrogen evolution catalysts.

We recently presented a computational strategy for the calculation of the reduction potentials and pK_a's of cobaloxime complexes using density functional theory (DFT).[11] In this scheme, the reaction free energy for reduction of a molecule in solution ($\Delta G_{solv}^{o,redox}$) is calculated in terms of the reaction free

Received: August 26, 2011
Published: October 27, 2011

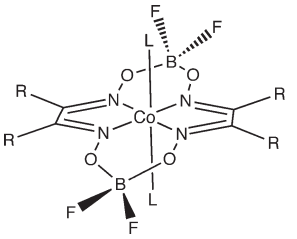

Figure 1. Schematic structure of the cobaloxime complex $Co(dRgBF_2)_2$.

Table 1. Substituents and Associated Hammett Constants[a]

−R	σ_p
−CN	0.66
$-CF_3$	0.54
−Cl	0.23
−H	0.00
$-C_6H_5$	−0.01
$-CH_3$	−0.17
$-OCH_3$	−0.27
−OH	−0.37
$-NH_2$	−0.66

[a] These Hammett constants describe the effects of para substitution on benzoic acid, as obtained from ref 15.

energy for reduction of the molecule in the gas phase ($\Delta G^{o,redox}_{gas}$) and the solvation free energies of the reduced and oxidized species [ΔG^{o}_{s}(Red) and ΔG^{o}_{s}(Ox), respectively] in a Born−Haber cycle:[12]

$$\Delta G^{o,redox}_{solv} = \Delta G^{o,redox}_{gas} + \Delta G^{o}_{s}(Red) - \Delta G^{o}_{s}(Ox) \quad (1)$$

Here $\Delta G^{o,redox}_{gas}$ is calculated from the Gibbs relation $\Delta G^{o,redox}_{gas} = \Delta H^{o,redox}_{gas} - T\Delta S^{o,redox}_{gas}$, which includes enthalpic contributions from zero-point energy and entropic contributions from vibrational frequencies at temperature T = 298.15 K. An analogous Born−Haber cycle is used for the calculation of pK_a's.[13] Reduction potentials are calculated according to the relation $E^o = -\Delta G^{o,redox}_{solv}/nF$, where F is the Faraday constant and n = 1 for the reactions studied. The pK_a is calculated from the associated reaction free energy in solution according to the relation $pK_a = \Delta G^{o,pK_a}_{solv}/[\ln(10)RT]$. All of the reduction potentials and pK_a's were calculated in acetonitrile.

We employed isodesmic reactions to calculate relative reduction potentials and pK_a's for a series of related complexes.[11] The use of isodesmic reactions with appropriate references accounts for systematic computational error in DFT calculations due to limitations in the basis sets and electron exchange−correlation functionals. This approach also eliminates the necessity of determining the free energies of the gas phase electron and proton, the solvation free energy of the proton, and the free energy of self-solvation associated with ligand loss[14] because these quantities cancel in the isodesmic reactions. In this communication, we are interested in the reduction potentials and pK_a's relative to the $Co(dmgBF_2)_2$ (dmg = dimethylglyoxime) complex. Thus, two reductions and a deprotonation of $Co(dmgBF_2)_2$ were used in the isodesmic reactions. The reference reactions, isodesmic reactions, and resulting equations for the reduction

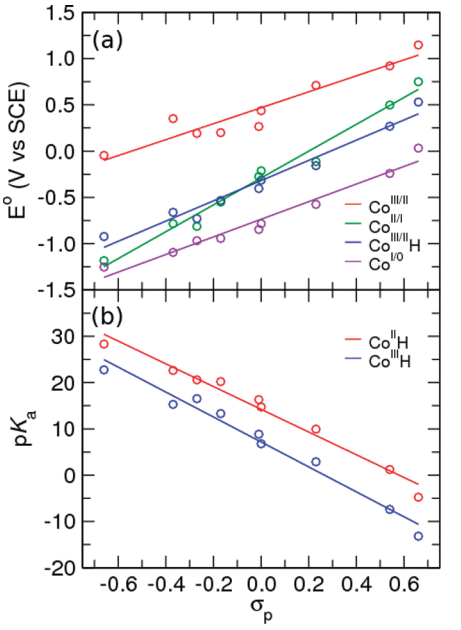

Figure 2. (a) Calculated reduction potentials $E^o(Co^{III/II})$, $E^o(Co^{II/I})$, $E^o(Co^{III/II}H)$, and $E^o(Co^{I/0})$ and (b) calculated pK_a's of $Co^{II}H$ and $Co^{III}H$ for $Co(dRgBF_2)_2$ as functions of the Hammett constants for the substituents R given in Table 1. The squares of the correlation coefficients are 0.905, 0.980, 0.966, 0.963, 0.976, 0.972, respectively.

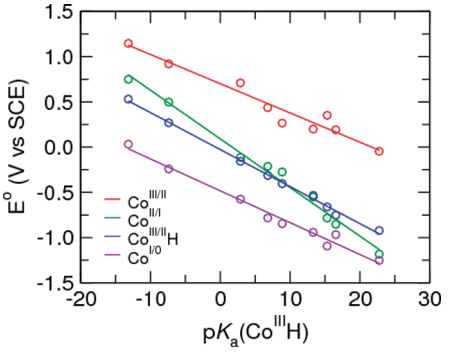

Figure 3. Linear correlations between the calculated reduction potentials $E^o(Co^{III/II})$, $E^o(Co^{II/I})$, $E^o(Co^{III/II}H)$, and $E^o(Co^{I/0})$ and the calculated $Co^{III}H$ pK_a values for $Co(dRgBF_2)_2$ for the substituents R given in Table 1. The squares of the correlation coefficients are 0.948, 0.990, 0.998, 0.981, respectively.

potentials and pK_a's are provided in eq S1 and Table S1 in the Supporting Information (SI).

The DFT calculations were performed using Gaussian 09.[16] Optimizations were performed in the gas phase at the B3P86/6-311+G** level of theory but using the smaller basis set 6-31G for the phenyl substituents. Solvation energies were calculated with the conductor-like polarizable continuum model using Bondi radii and including nonelectrostatic interactions resulting from dispersion, repulsion, and cavity formation. Benchmarking of this functional and basis set is provided in ref 17 and our previous work.[11] A summary of our benchmarking procedure is provided in Tables S2 and S3 in the SI.

The effects of the substituents R on the $Co^{III/II}$, $Co^{II/I}$, $Co^{III/II}H$, and $Co^{I/0}$ reduction potentials are depicted in Figure 2a. This figure illustrates a linear relationship between the reduction

dx.doi.org/10.1021/ja208091e |J. Am. Chem. Soc. 2011, 133, 19036–19039

potentials and the electron donating or withdrawing character of the substituents. The more strongly electron withdrawing groups are associated with more positive reduction potentials, while the more strongly electron donating groups are associated with more negative reduction potentials. This trend is expected on the basis of electrostatic considerations, as electron withdrawing groups more readily allow for reduction of the metal center. The pK_a values of $Co^{II}H$ and $Co^{III}H$ also change linearly with the Hammett constant, as depicted in Figure 2b. More strongly electron donating substituents decrease the propensity for the Co-hydride to lose a proton, thus increasing the pK_a, and the reverse trend is observed for electron withdrawing groups. Furthermore, Figure 3 illustrates a linear correlation between the $Co^{III/II}$, $Co^{II/I}$, $Co^{III/II}H$, and $Co^{I/0}$ reduction potentials and the $Co^{III}H$ pK_a. Similar linear correlations between the reduction potentials and the $Co^{II}H$ pK_a and between all pairs of these properties are observed. The calculated reduction potentials and pK_a's and the parameters used for the linear fits in Figures 2 and 3 are provided in Tables S4 and S5 in the SI.

In Figure 2, the lines associated with the reduction potentials of $Co^{II/I}$ and $Co^{III/II}H$ intersect at $\sigma_p \approx 0$. This figure is consistent with our previous analysis of cobaloximes with CH_3 substituents in ref 11. In that analysis, we proposed that the cyclic voltammogram peak observed experimentally at ca. −1.0 V vs SCE, which was tentatively assigned to the $Co^{III/II}H$ potential,[4] be reassigned to the $Co^{II/I}H$ potential. We also suggested that the peak corresponding to the $Co^{III/II}H$ potential is obscured by the peak corresponding to the $Co^{II/I}$ potential. On the basis of Figure 2, we predict that increasing or decreasing the Hammett constant of the substituent could separate the $Co^{III/II}H$ and $Co^{II/I}$ peaks in the cyclic voltammogram. For example, the CF_3 substituent would be a promising candidate for separating these two peaks.

The reduction potentials and pK_a values determine the free energy changes associated with the steps in the mechanistic pathways depicted in Scheme 1. The equations used to calculate these free energy changes are provided in Scheme S1 in the SI. To decrease the overpotential required for $Co^{II/I}$ reduction, which is the first step in all of the mechanisms in Scheme 1, more strongly electron withdrawing groups can be substituted on the diglyoxime ligands. To decrease the acid strength required for protonation of the cobaloxime catalyst, more strongly electron donating groups can be used to increase the pK_a of the $Co^{II}H$ and $Co^{III}H$ intermediates. It should be noted that increasing the $Co^{II/I}$ reduction potential requires electron withdrawing groups, while increasing the pK_a of $Co^{II}H$ or $Co^{III}H$ requires electron donating groups. Furthermore, these trends tend to be thermodynamically unfavorable for the hydrogen production step. Specifically, the hydrogen production step for all mechanisms becomes more exoergic at lower Co-hydride pK_a values and more negative reduction potentials. Thus, the catalysts must be finely tuned to balance the goals of minimizing the applied overpotential and acid strength without adversely affecting the hydrogen production step.

The specific experimental conditions dictate the optimal composition of the cobalt diglyoxime catalyst. To assist in the design of these catalysts, the reduction potentials and pK_a values can be used to generate free energy diagrams for the various mechanistic pathways. For example, a comparison of the free energy diagrams corresponding to the monometallic mechanisms in Scheme 1 for the cobaloximes having CH_3 and CF_3 substituents with tosic acid (*p*-toluenesulfonic acid) is depicted

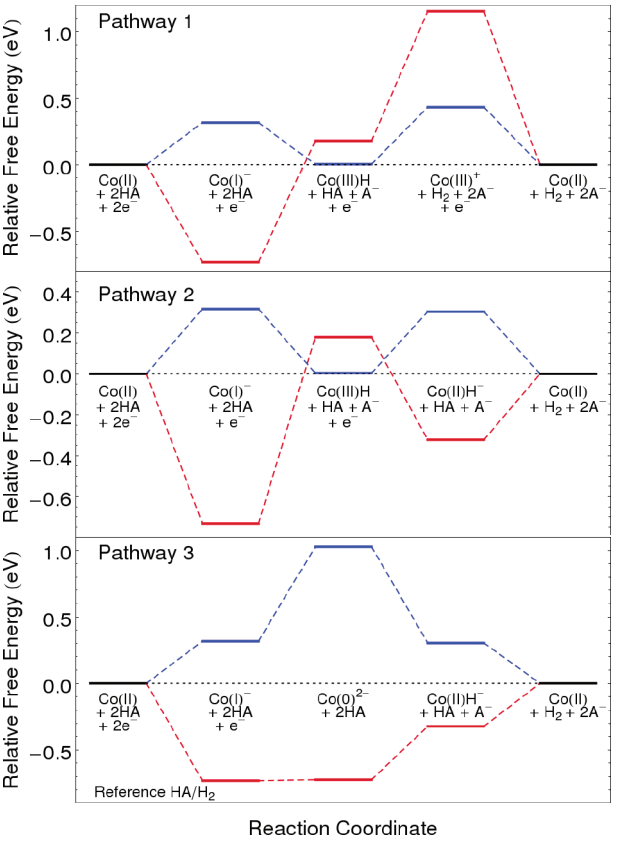

Figure 4. Thermodynamic free energy diagrams for monometallic pathways (1A, 2A, and 3A) for CH_3 substituents (blue lines) and CF_3 substituents (red lines). Relative free energies for half-reactions corresponding to electron transfer were calculated with respect to the HA/H_2 couple in acetonitrile, where HA is tosic acid (pK_a = 8.0). The free energy barriers are not shown.

in Figure 4. In this figure, the reference is the reduction potential for the HA/H_2 couple, $HA + e^- \rightarrow 1/2H_2 + A^-$, where HA is tosic acid (pK_a = 8.0 in acetonitrile) and $E^{o}_{HA/H_2} = -0.23$ V vs SCE.[4] Typically, catalysts should be designed to operate as close as possible to this reference potential to avoid high barriers and low minima.[18] In electrochemical experiments, H_2 evolution was found to occur at electrode potentials just negative of the $Co^{II/I}$ reduction potential.[2,4,5,7] Thus, the value of this reduction potential is another factor in catalyst design.

Figure 4 illustrates that the more strongly electron withdrawing CF_3 substituents yield more exoergic electron transfer steps and more endoergic proton transfer and hydrogen production steps in comparison with the CH_3 substituents. For the cobaloxime with CH_3 substituents, application of an overpotential equivalent to the $Co^{II/I}$ reduction potential will eliminate the free energy differences associated with the initial electron transfer steps in all pathways. For the cobaloxime with CF_3 substituents, the reduction from Co^{II} to Co^{I} does not require an applied overpotential, but the proton transfer and hydrogen production steps are less favorable. It should be noted that this thermodynamic analysis does not consider the free energy barriers, which impact the kinetics of these pathways. The analogous free energy diagrams for the bimetallic mechanisms in Scheme 1 are provided in Figure S1 in the SI. Similar free energy diagrams can be generated for all substituents with any choice of acid using the reduction potentials and pK_a's given in Figures 2 and 3.

To identify optimal cobaloxime catalysts, a function can be defined as the sum of the squared deviations of the points on the free energy diagram from the HA/H_2 reference potential for a specified mechanism. This function depends on the acid pK_a and the Hammett constant of the substituent. The minimum of this function with respect to the Hammett constant provides an indication of the optimal substituent for that specific acid and mechanism. The corresponding functions for the six mechanisms examined here are given in Table S6 in the SI. It should be noted that the free energy barriers are not considered in this analysis and could significantly impact the effectiveness of a catalyst. Moreover, certain steps could be weighted more than others in this procedure.

The free energy diagrams for all of the mechanisms in Scheme 1 may be used to identify the thermodynamically favorable pathways, and a comparison of these free energy diagrams for different substituents provides insight into the relative merits of these catalysts. The calculations of reduction potentials and pK_a's for these complexes are computationally expensive, however, and the investigation of a large number of catalysts with different substituents is not practical. The correlations identified in this communication enable the prediction of the reduction potentials and pK_a values with minimal calculations. If the Hammett constant for a particular substituent is known, the $Co^{III/II}$, $Co^{II/I}$, $Co^{III/II}H$, and $Co^{I/0}$ reduction potentials and the $Co^{II}H$ and $Co^{III}H$ pK_a values can be obtained from the linear relationships shown in Figure 2 using the corresponding parameters given in Table S5 in the SI. If the Hammett constant is not known, only one of these quantities must be calculated, and the other five quantities could be determined using the linear correlations between pairs of properties. The resulting reduction potentials and pK_a's may be used as input for the expressions given in Scheme S1 in the SI to generate the free energy diagrams for the various mechanistic pathways of the cobaloxime catalyst in conjunction with a specified acid and applied overpotential. Thus, these types of correlations will facilitate the computer-aided design of more effective cobaloxime catalysts for hydrogen evolution. In addition, this general approach could be applied to catalysts with other metal centers.

■ ASSOCIATED CONTENT

Supporting Information. Equations for free energy changes corresponding to the individual steps in the mechanistic pathways; isodesmic references, reactions, and equations used to calculate reduction potentials and pK_a's; comparison of calculated and experimental reduction potentials and pK_a's; calculated reduction potentials and pK_a's for the series of substituents; slopes and intercepts of linear fits; free energy diagrams comparing the bimetallic pathways for cobaloximes with CH_3 and CF_3 substituents; functions describing an optimal σ_p for each mechanism; complete ref 16; and coordinates and energies of optimized structures. This material is available free of charge via the Internet at http://pubs.acs.org.

■ AUTHOR INFORMATION

Corresponding Author
shs@chem.psu.edu

■ ACKNOWLEDGMENT

We are very grateful to Philip Hanoian and Alexander Soudackov for useful discussions and helpful advice. This work was supported by the NSF Center for Chemical Innovation (Powering the Planet, Grant CHE-0947829).

■ REFERENCES

(1) Connolly, P.; Espenson, J. H. *Inorg. Chem.* **1986**, *25*, 2684.
(2) Hu, X.; Cossairt, B. M.; Brunschwig, B. S.; Lewis, N. S.; Peters, J. C. *Chem. Commun.* **2005**, 4723.
(3) Razavet, M.; Artero, V.; Fontecave, M. *Inorg. Chem.* **2005**, *44*, 4786.
(4) Hu, X.; Brunschwig, B. S.; Peters, J. C. *J. Am. Chem. Soc.* **2007**, *129*, 8988.
(5) Baffert, C.; Artero, V.; Fontecave, M. *Inorg. Chem.* **2007**, *46*, 1817.
(6) (a) Du, P.; Knowles, K.; Eisenberg, R. *J. Am. Chem. Soc.* **2008**, *130*, 12576. (b) Du, P.; Schneider, J.; Luo, G.; Brennessel, W. W.; Eisenberg, R. *Inorg. Chem.* **2009**, *48*, 4952. (c) Lazarides, T.; McCormick, T.; Du, P.; Luo, G.; Lindley, B.; Eisenberg, R. *J. Am. Chem. Soc.* **2009**, *131*, 9192. (d) Szajna-Fuller, E.; Bakac, A. *Eur. J. Inorg. Chem.* **2010**, 2488.
(7) (a) Jacques, P.-A.; Artero, V.; Pécaut, J.; Fontecave, M. *Proc. Natl. Acad. Sci. U.S.A.* **2009**, *106*, 20627. (b) Dempsey, J. L.; Brunschwig, B. S.; Winkler, J. R.; Gray, H. B. *Acc. Chem. Res.* **2009**, *42*, 1995. (c) Dempsey, J. L.; Winkler, J. R.; Gray, H. B. *J. Am. Chem. Soc.* **2010**, *132*, 1060.
(8) Dempsey, J. L.; Winkler, J. R.; Gray, H. B. *J. Am. Chem. Soc.* **2010**, *132*, 16774.
(9) The photochemical experiments in ref 8 suggest that a transiently photogenerated $Co^{III}H$ complex is reduced by excess Co^{I} in solution to form $Co^{II}H$, which is subsequently protonated to produce H_2. This mechanism was not explicitly considered here but is consistent with the electrochemical pathway 2A. Other heterobimetallic pathways are also possible and could be analyzed with the data provided in this communication.
(10) Hammett, L. P. *J. Am. Chem. Soc.* **1937**, *59*, 96.
(11) Solis, B. H.; Hammes-Schiffer, S. *Inorg. Chem.* **2011**, *50*, 11252.
(12) (a) Roy, L. E.; Jakubikova, E.; Guthrie, M. G.; Batista, E. R. *J. Phys. Chem. A* **2009**, *113*, 6745. (b) Wang, T.; Brudvig, G. W.; Batista, V. S. *J. Chem. Theory Comput.* **2010**, *6*, 2395.
(13) Lim, C.; Bashford, D.; Karplus, M. *J. Phys. Chem.* **1991**, *95*, 5610.
(14) Kelly, C. P.; Cramer, C. J.; Truhlar, D. G. *J. Phys. Chem. B* **2007**, *111*, 408.
(15) Hansch, C.; Leo, A. *Substituent Constants for Correlation Analysis in Chemistry and Biology*; Wiley-Interscience: New York, 1979.
(16) Frisch, M. J.; et al. *Gaussian 09*, revision B.1; Gaussian, Inc.: Wallingford, CT, 2009.
(17) Qi, X.-J.; Fu, Y.; Liu, L.; Guo, Q.-X. *Organometallics* **2007**, *26*, 4197.
(18) Felton, G. A. N.; Glass, R. S.; Lichtenberger, D. L.; Evans, D. H. *Inorg. Chem.* **2006**, *45*, 9181.